Journal of
BIOPHOTONICS
3/13
www.biophotonics-journal.org

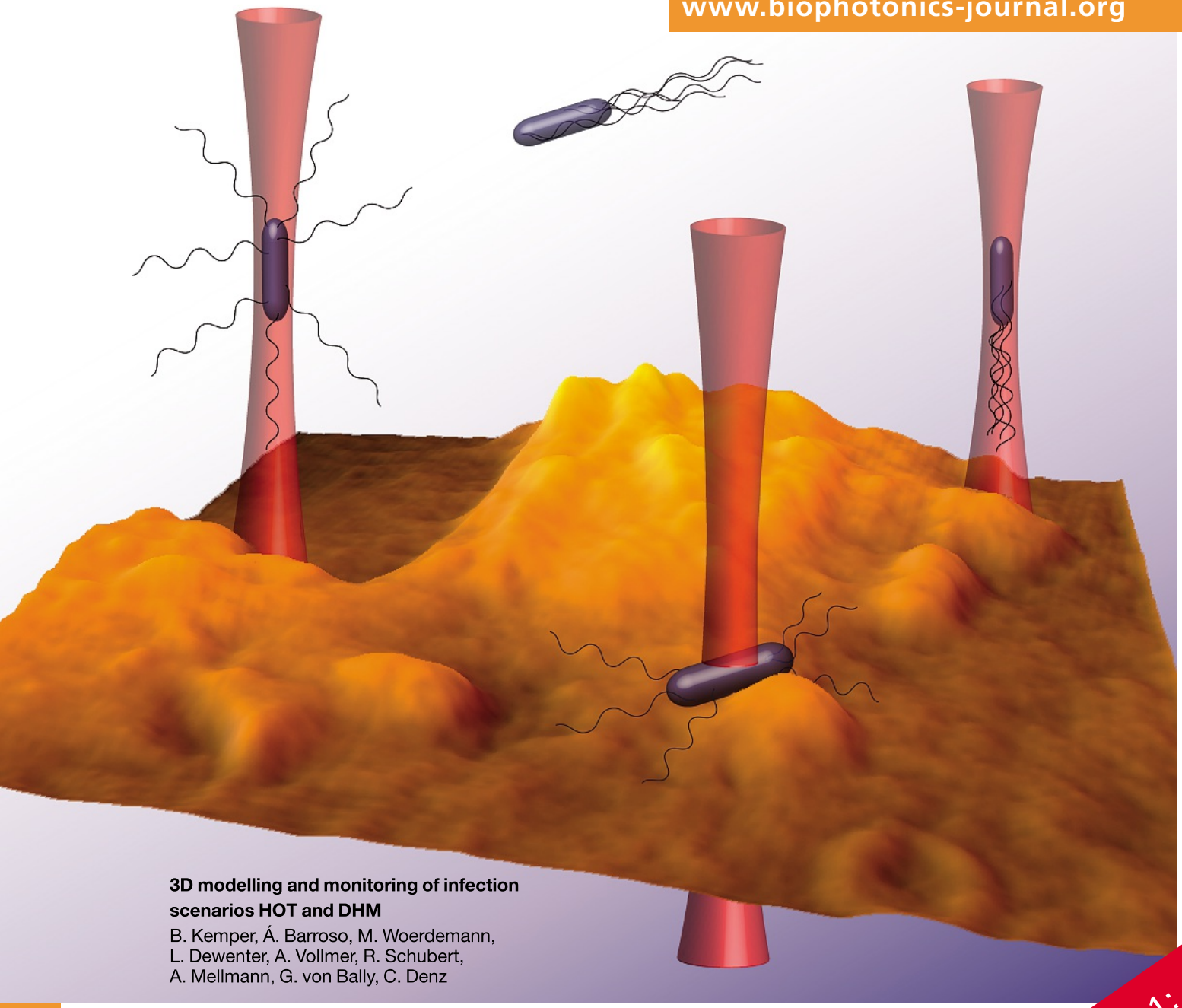

3D modelling and monitoring of infection scenarios HOT and DHM

B. Kemper, Á. Barroso, M. Woerdemann, L. Dewenter, A. Vollmer, R. Schubert, A. Mellmann, G. von Bally, C. Denz

WILEY-VCH

ISSN 1864-063X J. Biophotonics, Vol. **6**, No. 3 (March), 213–298 (2013)

Impact Factor 2011: **4.343**

J. Biophotonics **6**, No. 3, 260–266 (2013) / **DOI** 10.1002/jbio.201200057

Journal of BIOPHOTONICS

LETTER

Towards 3D modelling and imaging of infection scenarios at the single cell level using holographic optical tweezers and digital holographic microscopy

Björn Kemper[*,1], *Álvaro Barroso*[1,2], *Mike Woerdemann*[2], *Lena Dewenter*[2], *Angelika Vollmer*[1], *Robin Schubert*[1], *Alexander Mellmann*[3], *Gert von Bally*[1], *and Cornelia Denz*[2]

[1] Center for Biomedical Optics and Photonics, University of Muenster, Robert-Koch-Str. 45, 48149 Muenster, Germany
[2] Institute of Applied Physics, University of Muenster, Corrensstraße 2/4 Muenster, 48149 Muenster, Germany
[3] Institute of Hygiene, University of Muenster, Robert-Koch-Str. 41, 48149 Muenster, Germany

Received 28 March 2012, revised 25 May 2012, accepted 26 May 2012
Published online 12 June 2012

Key words: holographic optical tweezers, digital holographic microscopy, infection monitoring, live cell imaging, bacteria

Supporting information for this article is available free of charge under http://dx.doi.org/10.1002/jbio.201200057

The analysis of dynamic interactions of microorganisms with a host cell is of utmost importance for understanding infection processes. We present a biophotonic holographic workstation that allows optical manipulation of bacteria by holographic optical tweezers and simultaneously monitoring of dynamic processes with quantitative multi-focus phase imaging based on self-interference digital holographic microscopy. Our results show that several bacterial cells, even with non-spherical shape, can be aligned precisely on the surface of living host cells and localized reproducibly in three dimensions. In this way a new label-free multipurpose device for modelling and quantitative analysis of infection scenarios at the single cell level is provided.

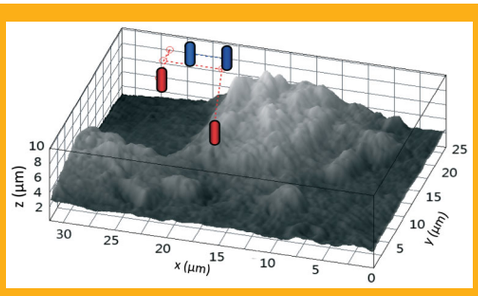

3D displacement trajectories of bacteria obtained by self-interference digital holographic microscopy during the optical manipulation with holographic optical tweezers. The data are superimposed to a topography map of a living tumour cell that results from the evaluation of the same holographically acquired measurement data.

1. Introduction

During the infection process, a host organism interacts with microorganisms such as viruses or bacteria. Typically, mammalian hosts react to infections with innate responses in which inflammation is often involved [1]. However, diagnosis of an infection can be difficult as sometimes specific signs and symptoms are absent. Thus, for a treatment with adequate pharmaceuticals, a clear diagnosis with a reliable identification of the microorganism and knowledge about the underlying infection mechanisms are crucial. For an efficient identification of infective agents, many different assays have been developed. Typical

* Corresponding author: e-mail: bkemper@uni-muenster.de

in vitro assays for bacteria are based on the cultivation in Petri dishes on solid media with subsequent phenotypic characterization or molecular techniques such as polymerase chain reactions (PCR) [2]. However, for a deeper understanding of the dynamics of infection processes, a quantitative, time-resolved analysis at the single cell level is necessary. Furthermore, the three-dimensional monitoring of interactions between the microorganisms and living host cells is of interest to elucidate different steps during the infection process, e.g. adherence on or invasion into the host cell. In order to design and analyze defined three-dimensional (3D) infection scenarios, methods are required that are capable of reliably manipulating and imaging single or multiple parasitic specimen and host cells. Ideally, these techniques should be minimally invasive in order to affect the processes of interest as little as possible. On the one hand, holographic optical tweezers (HOT) have been found suitable for the efficient 3D positioning and alignment of single and multiple bacteria and cells with laser light [3–5]. On the other hand, digital holographic microscopy (DHM) in off-axis configuration enables quantitative, minimally invasive multi-focus phase contrast imaging of biological samples by fast single-shot acquisition of digital holograms (see [6–10] and references therein) as well as the automated 3D tracking of living cells [11]. Exploiting the complementary features of both techniques, we combined both technologies into a single workstation, which we name "biophotonic holographic workstation", because both techniques are based on holography. In order to demonstrate in a proof-of-principle study the versatility of our workstation, we present for the first time to our knowledge 3D data from holographic manipulation and label-free quantitative imaging of model bacteria during a well-defined infection scenario to pancreatic tumor cells. Our approach provides new label-free equipment for modelling and quantitative dynamic 3D imaging of infection scenarios at a single cell level with hitherto unrivalled precision.

2. Methods and material

2.1 Holographic workstation

We combined a recently developed holographic optical tweezers system [4, 12] that is based on a phase-only spatial light modulator (SLM) with self-interference digital holographic microscopy [13]. Inspired from prior investigations on multi-modal imaging [14], the holographic workstation (Figure 1) was implemented on the basis of an inverted Nikon Ti microscope which was also equipped with an extension module for Nomarsky differential interference contrast (DIC) [15]. For optical manipulation, the light of a $Nd:YVO_4$ laser (Smart Laser Systems, Berlin, Germany, $\lambda_{HOT} = 1064$ nm, $P_{max} = 2500$ mW) was used. The laser light was collimated and directed via the SLM ("Pluto" LCOS display from Holoeye

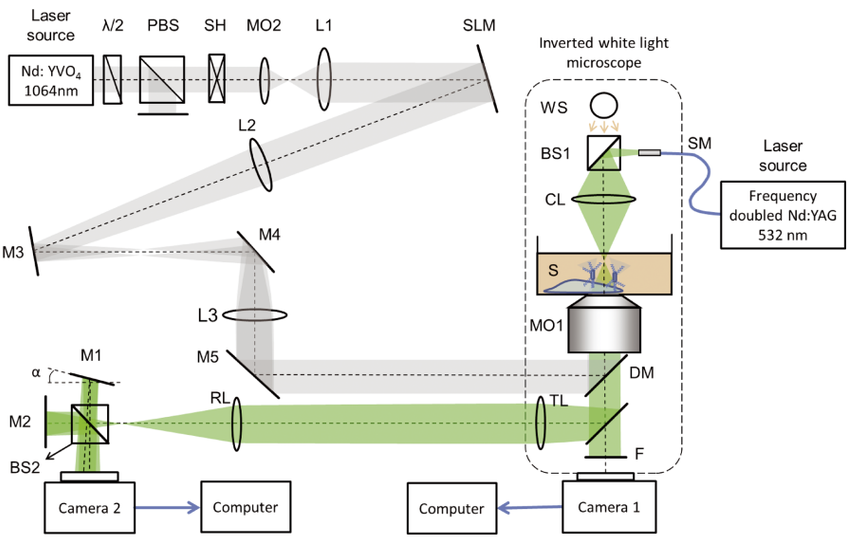

Figure 1 Sketch of the biophotonic holographic workstation consisting of spatial light modulator-based optical tweezers [4] and self-interference digital holographic microscopy [13]. $\lambda/2$: half wave plate; PBS: polarizing beam splitter cube; SH: shutter; MO1, MO2: microscope lenses; L1, L2, L3: lenses; WS: white light source: BS1, BS2: non polarizing beam splitter cubes; M1, M2, M3, M4: mirrors; F: filter; DM: dicroitic mirror; TL: tube lens; RL: relay lens; SM: single mode optical fiber; S: sample; CL: condenser lens; α: off-axis angle for self-interference DHM.

Journal of
BIOPHOTONICS

Photonics, Berlin, Germany) and appropriate relay optics to the back focal plane of an oil immersion microscope lens with a high numerical aperture (Nikon, 1.49) where a power of $P_{HOT} = 400$ mW was utilized to manipulate the specimens with one or multiple Gaussian shaped optical tweezers. In order to steer the tweezers, digital kinoforms were generated [16]. The software used was originally developed at the University of Glasgow, Scotland [17], and adapted to the specific requirements of the workstation. For quantitative phase imaging with DHM, a self-interference setup was adapted to one of the camera ports of the inverted microscope [13].

A frequency doubled Nd : YAG laser (Coherent, Compass 100, Lübeck, Germany, $\lambda_{DHM} = 532$ nm) was used as coherent light source. In difference to common Mach-Zehnder setups, a Michelson interferometer approach was used. Due to the short optical path length differences, this experimental setup is in particular insensitive to mechanical instabilities and vibrations. Off-axis digital holograms were created by a slight tilt (α) of one of the mirrors of the Michelson interferometer and were recorded by a CCD sensor (The Imaging Source DMK 41BU02, Bremen, Germany) which was also used for bright field imaging of the sample under white light illumination. The reconstruction of the resulting off-axis digital holograms was performed in two steps as reported in detail previously elsewhere [18–20]. First, the complex object wave was reconstructed by spatial phase shifting [18]. If the sample was not in focus during hologram recording, numerical refocusing by a convolution approach of the Huygens Fresnel principle was performed [19] in combination with a holographic autofocusing procedure [20].

2.2 Cells and bacteria

Based on experiences with the specimens from former experiments [4, 19] human pancreatic ductal adenocarcinoma cells (PaTu8988T [21]) were used to model the host in this proof-of-principle study while a wildtype strain of *Bacillus subtilis* (BD 630) was utilized as a model for the parasitic organism.

The PaTu8988T cells were obtained from the German Collection of Microorganisms and Cell Cultures (DSMZ, Braunschweig), Germany and cultured in Dulbecco's Modified Eagle Medium (DMEM) supplemented with 5% fetal calf serum (FCS), 5% horse serum, and 2 mM L-glutamine at 10% CO_2. For the experiments the medium was buffered with Hepes.

B. subtilis is a rod-shaped bacterium with a diameter of about 1 μm and a length of approximately 2.5 μm. For the experiments the bacteria were defrosted, centrifuged at 5000 g for 2–3 minutes, and resuspended at room temperature into chemotaxis buffer [22]. Then, the bacteria were suspended immediately to the cell culture buffer medium. Both, cells and bacteria, were studied in Petri Dishes (μ-Dish$^{35\,mm,low}$, ibidi GmbH, Munich, Germany). To avoid fast migrations of the tumor cells and possible overheating by the trapping laser beam the experiments were performed at room temperature ($T = 24$ °C) [23]. In order to prevent optical trapping of unwanted specimens a concentration of *B. subtilis* was chosen for which only few bacteria were visible within the field of view. Rod-shaped bacteria of this size and aspect ratio typically align their long axis with the beam axis in the employed configuration of discrete optical tweezers with Gaussian beam profile [24]. Using multiple optical tweezers acting at one bacterium, however, the orientation of the bacteria can be defined at will [4].

3. Results and discussion

Figure 2 shows an adherent PaTu8988T cell and two *B. subtilis* cells in different imaging modes. In the white light image (Figure 2a), the bacterial cells are only visible with low contrast, and it is difficult to distinguish them from intracellular organelles. In the corresponding differential interference contrast (DIC) image (Figure 2b) however, the morphology and the different orientations of the bacteria become clearly visible. The bacterium denoted with (1) is orientated in the x–y plane, while bacterium (2) is aligned along the z axis. Figure 2c shows a quantitative DHM phase image which quantifies the optical path length changes that are induced by the bacterial cells.

Although the image quality of the DHM phase contrast is lower than for DIC due to coherent scattering and parasitic interference patterns, the bacteria can be localized clearly as local maxima (see cross-sections plots in Figure 2d and e along the red and blue arrows in Figure 2c, respectively). The phase contrast of the rod-shaped *B. subtilis* (1) that was aligned in horizontal orientation and in parallel to the cell surface is lower than the phase retardation that is caused by bacterium (2) with orientation along the z axis. This demonstrates that the spatial alignment of the bacteria can be detected unambiguously by DHM phase contrast.

Figure 3 demonstrates the horizontal alignment of a bacterial cell to a host cell with HOT using a single optical trap by representative false colour coded quantitative DHM phase images (Figure 3a and b). The bacterium is clearly visible as a bright spot in each image (arrows in Figure 3a and b). The cross-sections in Figure 3c and d along the dotted lines in Figure 3a and b quantify the bacterium in-

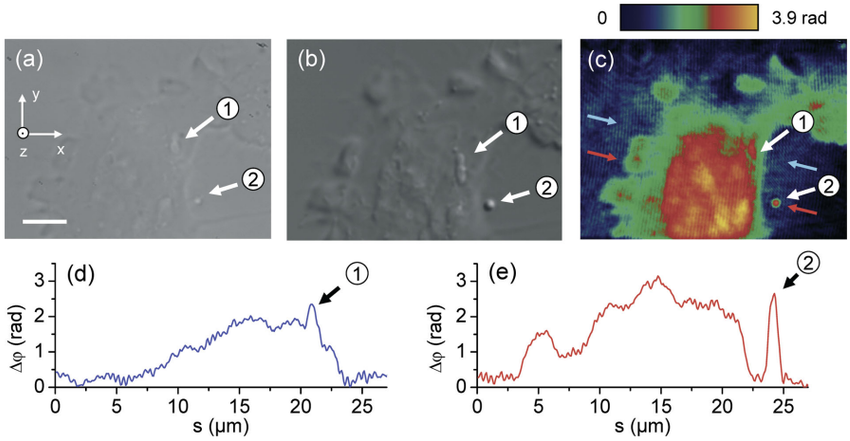

Figure 2 Imaging of a pancreatic tumor cell (PaTu8988T) and two *B. subtilis* cells (denoted as (1) and (2)) in different spatial orientations (white arrows) with different imaging modalities. (**a**): White light image; (**b**), (**c**): corresponding DIC and false colour coded quantitative DHM phase images; (**d**), (**e**): cross-sections through the DHM phase along the red and blue arrows in (**c**) that quantify the specimen induced phase retardation $\Delta\varphi$.
Scale bar: 5 μm

duced phase changes and also illustrate its lateral movement. The comparison of the local phase contrast maximum with the data from bacterium (2) in Figure 2c reveals that the HOT cause the specimen to align with the z axis. Furthermore, the comparison of the two cross-sections in Figure 3e show that the morphology of the cell does not change during optical manipulation of the bacteria with HOT. Thus, we conclude that no photo damage is induced during the observation time of about 10 min. In the further evaluation, the lateral coordinates of the maximum phase that is caused by the optically manipulated bacterium are determined as described in [11] in order to track its lateral two-dimensional (2D) motions.

Figure 3f depicts the resulting 2D displacement trajectory, obtained from a sequence of $N = 17$ subsequent quantitative DHM phase images, which is superimposed to a representative quantitative DHM phase map of the cell. Video 1 illustrates the dynamic tracking of the bacterium by a fast motion movie.

Having demonstrated dynamic 2D tracking, we investigated if dynamic 3D repositioning of multiple bacterial cells with HOT can be quantified by DHM. Therefore, within a timeframe of 30 s, $N = 110$ digital holograms of three bacterial cells were recorded. Initially the specimens were optically trapped in the same z plane, subsequently lifted up, and finally lifted down and brought to the surface of a PaTu8988T cell (for illustration see Figure 4a, b and

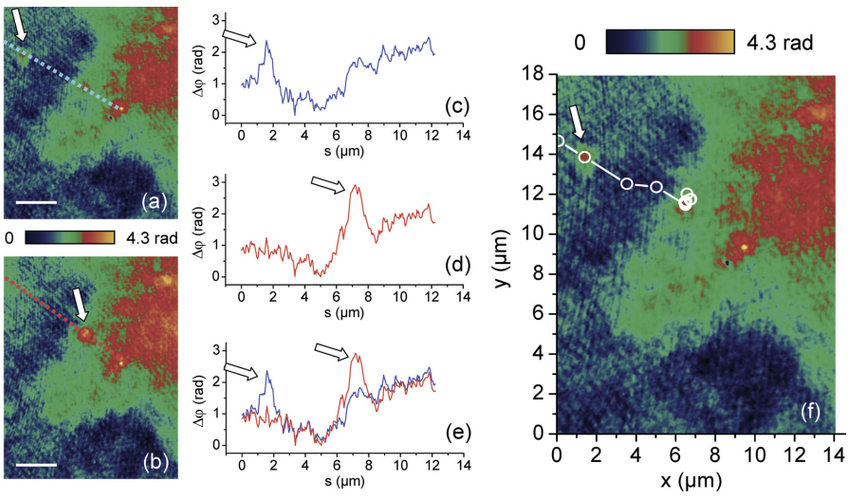

Figure 3 Automated 2D tracking of an optically-manipulated bacterium. (**a**), (**b**): false colour coded quantitative DHM phase images at $t = 0$ and at the time where the bacterium aligned on the cell surface; (**c**), (**d**): cross-sections through the cell and the bacterium along the dotted lines in (**a**) and (**b**); (**e**): comparative plot of the data in (**c**) and (**d**); (**f**): 2D displacement trajectory of the bacteria obtained from a sequence of $N = 17$ digital holograms superimposed to a representative quantitative phase image of the cell. The scale bar amounts to 5 μm (Video 1). The parameter $\Delta\varphi$ quantifies the specimen induced phase retardation.

Journal of
BIOPHOTONICS

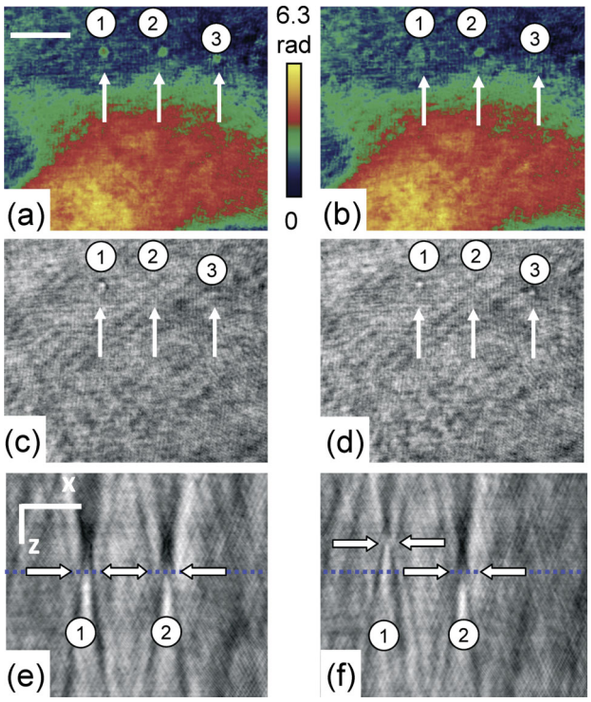

Figure 4 Representative images from the z localization of three *B. subtilis* cells (denoted with (1), (2), (3)) with DHM during dynamic manipulation with HOT. Left column: all bacteria are trapped in the same z plane, right column: bacteria (1) and (3) are lifted up by HOT; (**a**), (**b**): False color coded DHM phase images in the hologram plane; (**c**), (**d**): corresponding DHM amplitude images; (**e**), (**f**): cross-sections through numerically calculated focus stacks (x–z-plane) of amplitude images that demonstrate the lifting up of bacterium (1) relative to bacterium (2) (white arrows). The dashed blue line indicates the hologram plane. The scale bars correspond to 10 µm (x-axis) and 3 µm (z-axis). Video 2 illustrates the dynamic manipulation of the bacteria by a fast motion movie of quantitative DHM phase images.

Video 2). The DHM feature of subsequent numerical refocusing was used in the further evaluation to localize the axial position of the bacteria as described in detail in [11]. Figure 4e and f, show representative cross-sections through focus stacks of DHM amplitude images as depicted in Figure 4c and d (x–z plane). The amplitude images correspond to microscopic bright field images under coherent illumination and were generated from single digital off-axis holograms by numerical propagation of the object wave from the hologram plane to different image planes. The resulting image stacks visualize that bacterium (1) is lifted up by HOT relatively to bacterium (2). The 2D localisation of the bacteria was performed by evaluation of the sharply refocused quantitative phase images of the bacteria as illustrated in Figure 3.

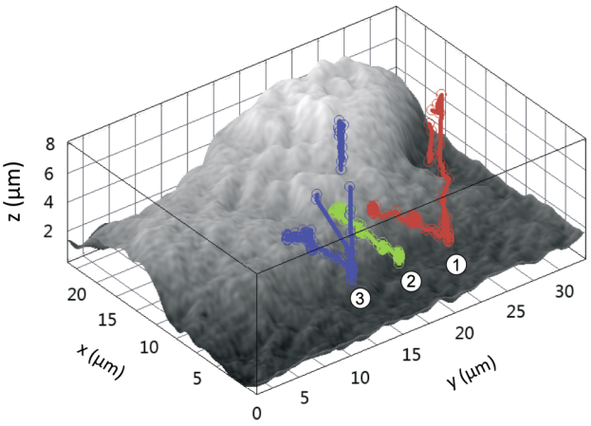

Figure 5 3D displacement trajectories of three bacterial cells determined from the data in Figure 4. The curves are superimposed to a gray level coded topography map of a living tumour cell which was calculated from a quantitative phase image that was obtained from digital hologram without bacteria within the field of view. Video 3 illustrates the 3D tracking process by a fast motion movie.

Figure 5 shows the resulting 3D displacement trajectories of all bacteria together with a topography map of the tumor cell. The topography map was obtained from a single digital hologram that was recorded without bacteria within the field of view. Therefore, the numerical reconstructed quantitative DHM phase image was evaluated as described in [19] using an integral cellular refractive index $n_{\mathrm{cell}} = 1.365$ (obtained from suspended PaTu8988T cells by a separate measurement [25]) and for a refractive index $n_{\mathrm{medium}} = 1.339$ of the cell culture medium. The disconnections within the 3D curves illustrate some missing data points that could not be evaluated due to disturbing light scattering effects and diffraction. However, the majority of 3D coordinates were successfully determined (bacterium (1): 95%, bacterium (2): 100%, bacterium (3): 95%). Video 3 illustrates the dynamics of the 3D tracking by a fast motion movie. The obtained trajectories demonstrate both, the reproducibility of 3D manipulation with HOT, and the reliable three-dimensional tracking of the bacteria with DHM. From the fluctuations of the 3D displacement trajectories, for all dimensions an average uncertainty of 0.3 µm for the bacterial localisation is determined. The symmetric resolution for the 3D localisation differs from the values that are expected by the numerical aperture of the used microscope lens. This may be explained by the influence of coherent noise (for illustration see Figures 3a, b, 4a, b) that is slightly higher for self-interference DHM than for Mach Zehnder interferometer-based setups [13] and thus lowers the accuracy for the lateral object localisation. As HOT allows stable trapping of bacteria for a certain time, in

future even higher accuracies for specimen localisation may be expected by enhancement of the DHM setup with synthetic aperture approaches, e.g., as proposed in [26, 27].

4. Conclusions

We have demonstrated that single and multiple bacteria can be simultaneously aligned and monitored in three dimensions by using a biophotonic holographic workstation that combines the complementary features of HOT and self-interference DHM. Bacterial cells with a size close to the diffraction limit of the employed optical imaging system are resolved in quantitative DHM phase contrast. The bacteria-induced signal in the quantitative phase images significantly exceeds the coherent noise in the utilized self-interference DHM setup. Thus, even different orientations of rod-shaped specimens are identified. Furthermore, it has been shown that bacteria can be reproducibly aligned on the surface of cells with sub micrometer accuracy. During the observation time no changes of the bacterial and cell morphology were observed in the quantitative DHM phase images. From this it can be concluded that the used optical tweezers system neither induced serious photo damage to the cells nor that the viability of the bacteria is significantly affected.

In conclusion, the concept of the presented biophotonic holographic workstation opens up bright future prospects for the modelling of infection scenarios. Bacteria can be minimally-invasively aligned on cells and localized precisely in three-dimensions. Moreover, it is possible to observe the interaction of bacteria and cells, and bacteria-induced cellular morphology changes quantitatively and label-free. Although further in-depth studies with suitable cellular and bacterial models are required, we believe that our approach paves the way towards innovative and substantial investigations of infection processes at the single cell level.

Acknowledgements This project was partly funded by the European Union Network of Excellence Photonics4Life (P4L). Further financial support by the German Ministry of Education and Research (BMBF) within the focus program "Biophotonics" (FKZ13N10937), the European Union funded Erasmus Program and the Medical Faculty of the University of Muenster (grant BD9817044) are gratefully acknowledged. The authors thank Christina Alpmann and Florian Hörner (Department of Applied Physics, University of Muenster, Germany) for helpful discussions, Christina Rommel and Jürgen Schnekenburger from the Biomedical Technology Center, University of Muenster, Germany, for support with the pancreatic tumor cells, and Berenike Maier and Jan Ribbe (both Biozentrum Köln, Universität zu Köln, Germany) for the kind supply of *B. subtilis* samples.

References

[1] S. Akira, Curr Top Microbiol Immunol. **311**, 1–16 (2006).
[2] S. Baron, Medical Microbiology. 4th ed., Galveston (TX) 1996.
[3] D. J. Stevenson, F. G. Moore, and K. Dholakia, J. Biomed. Opt. **15**, 041503 (2010).
[4] F. Hoerner, M. Woerdemann, S. Mueller, B. Maier, C. Denz, J. Biophoton. **3**, 468–475 (2010).
[5] G. Carmon, I. Fishov, and M. Feingold, Opt. Lett. **37**, 440–442 (2012).
[6] P. Marquet, B. Rappaz, P. J. Magistretti, E. Cuche, Y. Emery, T. Colomb, and C. Depeursinge, Opt. Lett. **30**, 468–470 (2005).
[7] B. Kemper and G. von Bally, Appl. Opt. **47**, A52–A61 (2008).
[8] M. K. Kim, SPIE Reviews **1**, 018005 (2010).
[9] G. Popescu, Quantitative phase imaging of cells and tissues (McGraw-Hill, New York, 2011).
[10] N. T. Shaked, M. T. Rinehart, and A. Wax, Quantitative phase microscopy of biological cell dynamics by wide-field digital interferometry, in: Coherent Light Microscopy for Imaging and Quantitative Phase Analysis (Springer, 2011), pp. 169–199.
[11] P. Langehanenberg, L. Ivanova, I. Bernhardt, S. Ketelhut, A. Vollmer, D. Dirksen, G. Georgiev, G. von Bally, and B. Kemper, J. Biomed. Opt. **14**, 014018 (2009).
[12] M. Woerdemann, S. Gläsener, F. Hörner, A. Devaux, L. D. Cola, and C. Denz, Adv. Mater. **22**, 4176–4179 (2010).
[13] B. Kemper, A. Vollmer, C. Rommel, J. Schnekenburger, and G. von Bally, J. Biomed. Opt. **16**, 026014 (2011).
[14] M. Esseling, B. Kemper, M. Antkowiak, D. Stevenson, L.Chaudet, M. A. A. Neil, P. W. French, G. von Bally, K. Dholakia, and C. Denz, J. Biophoton. **5**, 9–13 (2012).
[15] G. Nomarski, J. Phys. Radium **16**, 9–11 (1955).
[16] J. Liesener, M. Reicherter, T. Haist, and H. J. Tiziani, Opt. Commun. **185**, 77–82 (2000).
[17] R. W. Bowman, D. Preece, G. Gibson, and M. J. Padgett, J. Opt. A **13**, 044003 (2011).
[18] D. Carl, B. Kemper, G. Wernicke, and G. von Bally, Appl. Opt. **43**, 6536–6544 (2004).
[19] B. Kemper, D. Carl, J. Schnekenburger, I. Bredebusch, M. Schäfer, W. Domschke, and G. von Bally, J. Biomed. Opt. **11**, 034005 (2006).
[20] P. Langehanenberg, B. Kemper, D. Dirksen, and G. von Bally, Appl. Opt. **47**, A52–A61 (2008).
[21] H. P. Elsässer, U. Lehr, B. Agricola, and H. F. Kern, Virchows Arch. B **61**, 295–306 (1992).
[22] G. Ordal and D. Goldman, Science **189**, 802–805 (1975).

[23] A. Barroso, B. Kemper, M. Woerdemann, A. Vollmer, S. Ketelhut, and G. von Bally, C. Denz, Proc. SPIE **8427**, 84270A (2012).
[24] L. Dewenter, C. Alpmann, M. Woerdemann, and C. Denz, Proc. SPIE **8427**, 84270N (2012).
[25] B. Kemper, S. Kosmeier, P. Langehanenberg, G. von Bally, I. Bredebusch, W. Domschke, and J. Schnekenburger, J. Biomed. Opt. **12**, 054009 (2007).
[26] M. Debailleul, V. Georges, B. Simon, R. Morin, and O. Haeberlé, Opt. Lett. **34**, 79–81 (2009).
[27] M. Kim, Y. Choi, C. Fang-Yen, Y. Sung, R. R. Dasari, M. S. Feld, and W. Choi, Opt. Lett. **36**, 148–150 (2011).

